

Effect of Ionic Liquids on the Menshutkin Reaction: An Experimental and Theoretical Study

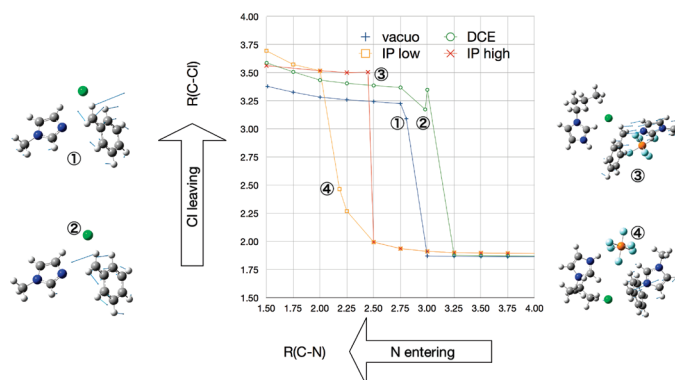
Riccardo Bini,[†] Cinzia Chiappe,* Christian Silvio Pomelli,* and Benedetta Parisi

Dipartimento di Chimica e Chimica Industriale, via Risorgimento 35, 56126 Pisa, Italy.

[†]*Present address: Dipartimento di Scienze Chimiche, via Marzolo 1, 35131 Padova, Italy.*

cinziac@farm.unipi.it; cris@dcc.unipi.it

Received May 5, 2009



The effect of ionic liquids (ILs) on the Menshutkin reaction between *N*-methylimidazole and benzyl halides has been investigated. Hammett correlations have been used to obtain information on the reaction mechanism of benzyl chlorides in ionic and molecular solvents. The solvent effects on this reaction have been examined using both multiparameter linear solvation energy relationships and theoretical calculations. These latter have been performed using a supermolecular approach, i.e., the IL is represented by an explicit ionic pair, IP. Two possible different reaction pathways have been obtained changing the position of the IL-IP with respect to the reagents. It is hypothesized that inside the IL the Menshutkin reaction of benzyl chloride with *N*-methylimidazole can follow different reaction pathways by considering the influence of dynamic heterogeneity in ionic media on the time scale of the lifetime of a transition state.

Introduction

Room temperature ionic liquids (ILs) have attracted considerable attention in recent years due to their unique physical and chemical properties and the facility by which many of these properties may be varied.¹ They are now being explored in virtually all areas of chemistry, as solvents for organic and inorganic reactions or (bio)catalyzed processes, as electrolytes in batteries and solar cells, and as new materials. Various physical properties of ILs, necessary to facilitate the use of ILs for these applications, have been

measured and collected,² but the number of ILs characterized completely is still limited. The number of studies performed to understand the structure of ionic liquids and the effect of ILs on reaction rate and selectivity is also limited.^{3,4}

(1) *Ionic Liquids IIIB: Fundamentals, Progress, Challenges, and Opportunities—Transformations and Processes*; Rogers, R. D., Seddon, K. R., Eds.; ACS Symposium Series 902; American Chemical Society: Washington DC, 2005. *Ionic Liquids IIIA: Fundamentals, Progress, Challenges, and Opportunities—Properties and Structure* Rogers, R. D., Seddon, K. R., Eds.; ACS Symposium Series 901; American Chemical Society: Washington, DC, 2005. *Ionic Liquids in Synthesis*, 2nd ed.; Wasserscheid, P., Welton, T., Eds.; Wiley-VCH: Weinheim, 2008.

(2) Chiappe, C.; Pieraccini, D. *J. Phys. Org. Chem.* **2005**, *18*, 275.

(3) (a) Lancaster, N. L.; Welton, T. *J. Org. Chem.* **2004**, *69*, 5986. (b) Anderson, J. L.; Ding, J.; Welton, T.; Armstrong, D. W. *J. Am. Chem. Soc.* **2002**, *124*, 14247. (c) Crowhurst, L.; Lancaster, N. L.; Perez Arlandis, J. M.; Welton, T. *J. Am. Chem. Soc.* **2004**, *126*, 11549. (d) Lancaster, N. L.; Salter, P. A.; Welton, T.; Young, G. B. *J. Org. Chem.* **2002**, *67*, 8855. (e) Chiappe, C.; Pieraccini, D. *J. Org. Chem.* **2004**, *69*, 6059. (f) Grodkowski, J.; Neta, P.; Wishart, J. F. *J. Phys. Chem. A* **2003**, *107*, 9794. (g) Skrzypczak, A.; Neta, P. *J. Phys. Chem. A* **2003**, *107*, 7800. (h) D'Anna, F.; Frenna, V.; Noto, R.; Pace, V.; Spinelli, D. *J. Org. Chem.* **2006**, *71*, 5144. (i) Chiappe, C.; Pieraccini, D.; Sullo, P. *J. Org. Chem.* **2003**, *68*, 6710. (l) Bini, R.; Chiappe, C.; Pieraccini, D.; Piccioli, P.; Pomelli, C. S. *Tetrahedron Lett.* **2005**, *46*, 6675. (m) Crowhurst, L.; Falcone, R.; Lancaster, N. L.; Llopsi-Mestre, V.; Welton, T. *J. Org. Chem.* **2006**, *71*, 8847. (n) Hallet, J. P.; Liotta, C. L.; Ranieri, G.; Welton, T. *J. Org. Chem.* **2009**, *74*, 1864. (o) Bini, R.; Chiappe, C.; Llopsi-Mestre, V.; Pomelli, C. S.; Welton, T. *Org. Biomol. Chem.* **2008**, *6*, 2522. (4) Harper, J. B.; Kobrak, M. N. *Mini-Rev. Org. Chem.* **2006**, *3*, 253.

TABLE 1. Solvent Parameters¹³

solvent	H bond donor acidity, α	H bond acceptor basicity, β	dipolarity/polarizability, π^*	cohesive pressure, δ^2 (J cm ⁻³)	permittivity, ϵ
acetonitrile	0.190	0.310	0.750	590	35.9
<i>N,N</i> -dimethylformamide	0.000	0.690	0.880	164	36.7
[bmim][PF ₆]	0.634	0.207	1.032	718	11.4
[bmim][Tf ₂ N]	0.617	0.243	0.984	554	11.6
[bm ₂ im][Tf ₂ N]	0.381	0.239	1.010	625	
[bmpyrr][Tf ₂ N]	0.427	0.252	0.954	506	11.7

Composed exclusively by ions, ILs differ significantly from water and organic solvents. The strong ion–ion interactions present in ILs lead to highly structured materials, three-dimensional polymeric networks of anions and cations linked by H-bonds and/or Coulombic interactions, often characterized by the presence of polar and nonpolar regions.⁵ In the case of imidazolium-based ionic liquids, the most investigated ILs, the existence of dynamic heterogeneous environments have been reported; molecules are trapped for a relatively long period in quasistatic local solvent cages.⁶ This trapping time, which is longer than in molecular solvents, together with the inability of the surroundings to adiabatically relax, induces a set of site-specific spectroscopic responses (excitation-wavelength-dependent fluorescence spectrum).⁷ Although in principle this heterogeneity might also affect reactivity, rarely has a hypothesis about the consequences of these structural features on reaction rate and/or selectivity been made. The effect of dynamic heterogeneity on reaction rates have been considered only for very fast reactions.⁸ Generally, the kinetic behavior of homogeneous reactions carried out in ILs have been rationalized in terms of transition state theory; the solvent modifies the Gibbs energy of activation by differential solvation of reactants and the activated complex, considering that solvent averaging occurs in a sufficiently short time to guarantee the absence of any heterogeneity.

Here, we report on the IL solvent effect on Menshutkin reaction, i.e., the quaternization of a tertiary amine (*N*-methylimidazole) by benzyl halides. The reaction is formally an alkyl group transfer,⁹ a process of central importance in biochemistry and a widely used strategy in organic synthesis; it is the reaction generally used to prepare ILs. Numerous physical organic studies have been conducted on the Menshutkin reaction,¹⁰ and it is a useful test system for theoretical methods.¹¹ Moreover, a recent study by Neta et al.¹² on the kinetic behavior of the Menshutkin reaction of 1,2-dimethylimidazole with benzyl bromide has shown that the reaction is moderately affected by the ionic medium, although

the process is characterized by an increase of charge on going from reagents to the transition state (TS). This result is quite surprising, especially if we consider that the monopolar charge character of the constituent ions of ILs should lead to substantial solvation stabilization of the charged Menshutkin TS. This paper investigates this behavior in more depth.

Results and Discussion

Effect of Solvent on Reaction Rate. The Menshutkin substitution reaction of *N*-methylimidazole and benzyl halides (Scheme 1) has been investigated in two molecular solvents (acetonitrile and *N,N*-dimethylformamide) and four ILs (1-butyl-1-methylpyrrolidinium bis(trifluoromethanesulfonyl)imide [bmpy][Tf₂N], 1-butyl-3-methylimidazolium bis(trifluoromethanesulfonyl)imide [bmim][Tf₂N], 1-butyl-2,3-dimethylimidazolium bis(trifluoromethanesulfonyl)imide [bm₂im][Tf₂N], and 1-butyl-3-methylimidazolium hexafluorophosphate [bmim][PF₆]), each having different macro- and microscopic physicochemical properties (Table 1).¹³

The kinetic measurements were carried out by following the disappearance of the benzyl halides at selected wavelengths between 260 and 300 nm, well above the cutoff of the ILs used as solvents (240 and 200 nm for imidazolium-based and pyrrolidinium-based ILs, respectively). The experiments were performed under pseudo-first-order conditions, using a large excess of *N*-methylimidazole, in a temperature range between 290 and 330 K. Kinetic data (absorbances vs time) were fitted with the exponential eq 1:

$$A(t) = A_{\text{inf}} + (A_0 - A_{\text{inf}}) \exp(-k_{\text{obs}}t) \quad (1)$$

where $A(t)$ is the absorbance at time t , A_{inf} is the absorbance at the final time, A_0 is the absorbance at the initial time and k_{obs} is the observed rate constant.

Nucleophilic substitution reactions, occurring through mono- and bimolecular processes (S_N1 and S_N2), are generally described by eq 2:

$$-d[\text{substrate}]/dt = [\text{substrate}][k_2[\text{nucleophile}] + k_1] \quad (2)$$

However, under the pseudo-first-order conditions (large excess of nucleophile) employed in this study, k_{obs} may be defined as

$$k_{\text{obs}} = k_2[\text{nucleophile}] + k_1 \quad (3)$$

(5) Lopes, J. N. A.; Padua, A. A. H. *J. Phys. Chem B* **2006**, *110*, 3330. Chiappe, C. *Monatsh. Chem.* **2007**, *137*, 1035. Xiao, D.; Rajian, J. R.; Hines, L. G.; Li, S.; Bartsch, R. A.; Quitevis, E. L. *J. Phys. Chem B* **2008**, *112*, 13316. Consorti, C. S.; Suarez, P. A. Z.; de Souza, R. F.; Burrow, R. A.; Farrar, D. H.; Lough, A. J.; Loh, W.; da Silva, L. H. M.; Dupont, J. *J. Phys. Chem. B* **2005**, *109*, 4341.

(6) Hu, Z.; Margulis, C. J. *Proc. Natl. Acad. Sci. U.S.A.* **2006**, *103*, 831. (7) Mandal, P.; Sarkar, M.; Samanta, A. *J. Phys. Chem. A* **2004**, *108*, 9048.

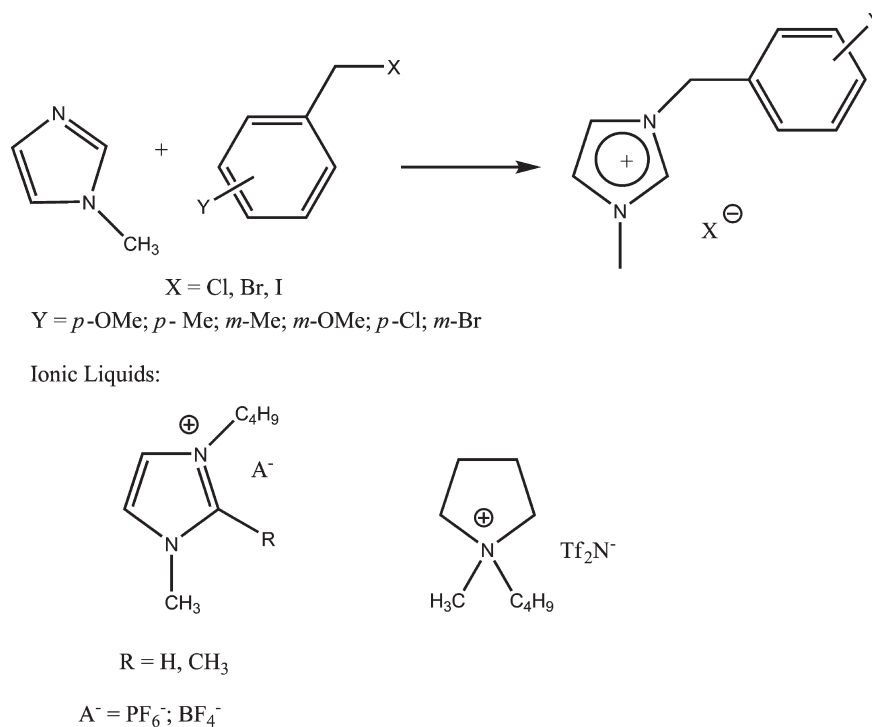
(8) Shim, Y.; Jeong, D.; Manjari, S.; Choi, M. Y.; Kim, H. *J. Acc. Chem. Res.* **2007**, *40*, 1130. Jin, H.; Li, X.; Marocelli, M. *J. Phys. Chem. B* **2007**, *111*, 13473.

(9) Menshutkin, N. Z. *Phys. Chem.* **1890**, *6*, 41. (10) Abboud, J. L. M.; Notario, R.; Bertran, J.; Sola, M. *Prog. Phys. Org. Chem.* **1993**, *19*, 1.

(11) Castejon, H.; Wiberg, K. B. *J. Am. Chem. Soc.* **1999**, *121*, 2139.

(12) Skrzypczak, A.; Neta, P. *Int. J. Chem. Kinet.* **2004**, *36*, 253.

(13) (a) Wakai, C.; Oleinokova, A.; Ott, M.; Weingartner, H. *J. Phys. Chem. B* **2005**, *109*, 17028. (b) Weingartner, H.; Sasisanker, P.; Dagenet, C.; Dyson, P. J.; Krossing, I.; Slatery, J. M.; Schubert, T. *J. Phys. Chem. B* **2007**, *111*, 4775. (c) Reichardt, C. *Green Chem.* **2005**, *7*, 339. (d) Crowhurst, L.; Mawdsley, P. R.; Perez-Arlandis, J. M.; Salter, P. A.; Welton, T. *Phys. Chem. Chem. Phys.* **2003**, *5*, 2790. Angelini, G.; Chiappe, C.; De Maria, P.; Fontana, F.; Gasparrini, D.; Pieraccini, D.; Pierini, M.; Siani, G. *J. Org. Chem.* **2005**, *70*, 8193. Kamlet, M. J.; Abboud, J.-L. M.; Abraham, M. H.; Taft, R. W. *J. Org. Chem.* **1983**, *48*, 2877.

SCHEME 1. Menshutkin Reaction between *N*-Methylimidazole and Benzyl Halides

where [nucleophile] is the molar concentration of *N*-methylimidazole ([NMI]), k_2 is the rate constant of the bimolecular reaction (S_N2), and k_1 is the rate constant of the monomolecular reaction, S_N1. Shown in Figure 1 is a plot of k_{obs} versus [NMI] for the reaction of *p*-methoxybenzyl chloride in [bm₂im][Tf₂N] at 333 K. Similar linear plots ($R > 0.999$) were obtained for all investigated benzyl halides in ILs and molecular solvents. In all of these plots, the intercept value was always close to zero, evidence that the monomolecular (S_N1) contribution to the reaction mechanism could be excluded. The second order rate constants, k_2 , determined from the slope values are reported in Tables 2 and 3.

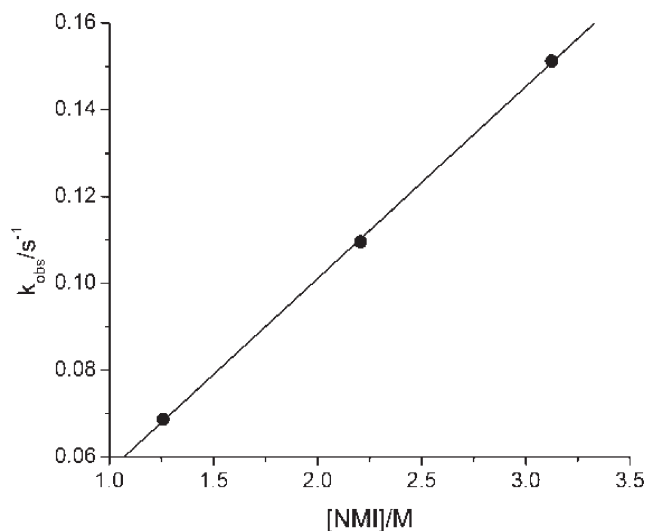


FIGURE 1. Plot of k_{obs} against [NMI] for the reactions of *p*-methoxybenzyl chloride and NMI in [bm₂im][Tf₂N] at 333 K.

According to the data shown in Table 2, the reactivity scale as a function of the leaving group follows the order BzI > BzBr \gg BzCl, both in molecular solvents and in [bmim][Tf₂N]. In contrast, BzBr is more reactive than BzI in [bmim][PF₆]. Furthermore, it is noteworthy that in the case of benzyl iodide rate constants are higher in organic solvents than in ILs, whereas the opposite trend characterizes the reaction of benzyl chloride. On the other hand, very similar rate constants were determined in all of the investigated solvents in the case of benzyl bromide. A very small solvent effect was also observed¹² in the reaction of 1,2-dimethylimidazole with benzyl bromide. Therefore, although on the basis of the kinetic constants found for benzyl iodide a trend qualitatively in agreement to the Hughes-Ingold rules might be envisaged (i.e., reactivity increases with increasing permittivity), this model is unable to explain the reactivity of BzCl and BzBr.

TABLE 2. Second-Order Rate Constants for the Reaction between *N*-Methylimidazole and Benzyl Halides in Molecular and Ionic Solvents at 298 K

solvent	$k_2 \times 10^4 \text{ (M}^{-1} \text{ s}^{-1}\text{)}$		
	benzyl iodide	benzyl bromide	benzyl chloride
acetonitrile	31.6(0.2)	11.10(0.2)	0.074(0.005)
<i>N,N</i> -dimethylformamide	55.20(0.2)	1.34(0.02)	0.075(0.005)
[bmim][Tf ₂ N]	26.70(0.5)	15.5(0.5)	0.146(0.005)
[bmim][PF ₆]	15.4(0.4)	20.3(0.4)	0.236(0.005)

To obtain more information about the ability of the ionic media to affect reactivity in the Menshutkin reaction, the kinetic behavior of the reaction of benzyl chloride was investigated in two other ILs, [bm₂im][Tf₂N] and [bmpyrr][Tf₂N],

TABLE 3. Second-Order Rate Constants for the Reaction between *N*-Methylimidazole and Various Substituted Benzyl Chlorides in Various Solvents at 333 K

solvents	$k_2 \times 10^4 \text{ (M}^{-1} \text{ s}^{-1})^a$						
	H	<i>p</i> -MeO	<i>m</i> -MeO	<i>p</i> -Me	<i>m</i> -Me	<i>p</i> -Cl	<i>m</i> -Br
acetonitrile	0.97	2.92	0.99	1.38	1.48	1.07	1.15
<i>N,N</i> -dimethylformamide	1.52	2.54	1.18	1.51	1.04	1.31	1.45
[bmim][Tf ₂ N]	2.44	11.9	1.98	5.30	2.98	1.85	1.66
[bmim][PF ₆]	3.64	16.8	3.96	6.53	5.06	3.92	4.79
[bm ₂ im][Tf ₂ N]	2.18	7.37	no reaction	2.87	2.35		
[bmpyrr][Tf ₂ N]	3.77	5.04	no reaction	2.74	no reaction		

^aStandard deviations were always less than 10%.

each having a different hydrogen bond donor acidity, α . Furthermore, we checked the kinetic effects arising from the introduction of electron-withdrawing or -donating substituents (EWS or EDS) on the benzylic moiety in the *meta* and *para* positions. Due to the low reactivity of benzyl chlorides bearing EWS these latter kinetic measurements were carried out at 333 K (Table 3).

In all cases, reactivity increases on going from molecular solvents to ILs. This behavior is however more evident for benzyl chlorides bearing EDS in a *para* position, whose reactivity significantly increases in the ILs having the higher hydrogen bond acidity, α . Fairly good linear relationships ($R^2 > 0.99$, in both cases) have been obtained plotting the $\log k_2$ values found for *p*-methoxybenzyl chloride or *p*-methylbenzyl chloride against the α parameter. In contrast, attempts to correlate the kinetic constants of the unsubstituted benzyl chloride to α or any other solvent properties using single parameter relationships gave always poor correlations. Therefore, the solvent dependent property $\log k_2$ was modeled applying a multiparameter relationship (LSER)¹⁴ of the type of eq 4, using different combinations of the parameters reported in Table 1:

$$\log k_2 = \text{const} + a\alpha + b\beta + c\pi^* + d\delta - \delta + e\epsilon + \dots \quad (4)$$

The best fit ($R^2 = 0.997$, F -term = 71) was obtained by a combination of α , β , π^* and δ :

$$\log k_2 = -1.24(0.42) + 0.44(0.15)\alpha - 2.62(0.3)\beta + 0.64(0.21)\pi^* - 0.10(0.01)\delta$$

Although the limited number of data (six kinetic constants) compared with the number of used parameters (four) reduces the validity of the procedure and the error associated with each parameter is quite high (in particular in the case of α and π^*), we believe that some considerations are feasible. Parameters β and δ appear as the most significant. However, since attempts to fit the experimental data using just these two parameters gave a very poor correlation ($R^2 = 0.782$, F -term = 5), also α and π^* play a not negligible role. Considering that the coefficients of α and π^* are positive, the correlation suggests that an increase in polarizability/dipolarity and in the hydrogen-bond donating ability of the solvent (this latter property primarily due to the IL cation)¹³ increase the rate of the reaction. This may be rationalized by considering that both of these parameters may favor the departure of the leaving group (in this case a chloride anion). This effect surmounts the attenuation of the nucleophilicity of the amine (NMI) due to the hydrogen bonding ability of the solvent, a behavior already observed in ILs having large

α values. In contrast, the regression indicates that an increase in the β and δ parameters decreases reactivity. This behavior can be explained by considering that in ILs the possibility for cations or anions to interact with a solute is always in competition with the cation–anion interactions present in the bulk ILs. Since, the hydrogen bond acceptor property of ILs is mainly related to the anion, ILs having higher values of β are characterized by stronger cation anion interactions; this feature reduce the ability of IL components (cations and/or anions) to interact with dissolved species.

Effect of Substituents on Reaction Rate. Important information about the mechanism of this reaction in ILs has been obtained also by analyzing the kinetic data of substituted benzyl chlorides through the application of the Hammett correlation, described by eq 5:¹⁵

$$\log \frac{k}{k_0} = \sigma\rho \quad (5)$$

Here, k_0 is the rate constant of the reference reaction (i.e., the reaction of benzyl chloride ($X = H$)), σ represents the electronic effect of the substituent on the reaction rate, and ρ is the sensitivity of the reaction toward the substituent change. Generally, the magnitude of ρ is related to the extent of the charge density in the transition state and whether the activated complex has anionic or cationic character. Briefly, $\rho < 0$ means that the activated complex bears a partial positive charge and $\rho > 0$ a negative one. Hammett plots for the reaction between NMI with benzyl chlorides in two organic solvents and two ILs at 333 K are reported in Figure 2. Poor linear correlations have been found both in organic solvents and ILs. On the other hand, attempts to correlate the rate constants with σ^+ parameters gave even poorer correlations.

Although to the best of our knowledge Hammett correlations have never been reported for reactions in ILs, nonlinear or bent plots have been obtained¹⁶ for many organic reactions in molecular solvents. Generally, this behavior is attributed to variations in the rate-determining step¹⁷ and, in the specific case of the Menschutkin reaction, to shifts in the TS position.

Although the distinction between monomolecular (S_N1) and bimolecular (S_N2) mechanisms for nucleophilic substitution reactions has represented starting from the work of Ingold¹⁸ a milestone in the development of organic

(14) Kamlet, M. J.; Abboud, J. L. M.; Abraham, M. H.; Taft, R. W. *J. Org. Chem.* **1983**, *48*, 2877.

(15) Anslyn, E. V.; Dougherty, D. A. *Modern Physical Organic Chemistry*, 1st ed.; University Science Books: Sausalito, CA, 2006. Wakai, C.; Oleinikova, A.; Ott, M.; Weingärtner, H. *J. Phys. Chem. B* **2005**, *109*, 17028.

(16) Carroll F. A. *Structure and Mechanism in Organic Chemistry*; Brooks/Cole Publishing Company: Pacific Grove, CA, 1998.

(17) Hill, J. W.; Fry, A. J. *Am. Chem. Soc.* **1962**, *84*, 2763. Lim, C.; Kim, S. H.; Yoh, D.-D.; Fujio, M.; Tsuno, Y. *Tetrahedron Lett.* **1997**, *38*, 3243. Lee, I.; Koo, S. *Tetrahedron* **1983**, *39*, 1803.

(18) Ingold, C. K. *Structure and Mechanism in Organic Chemistry*, 2nd ed.; Cornell University Press: Ithaca, 1969.

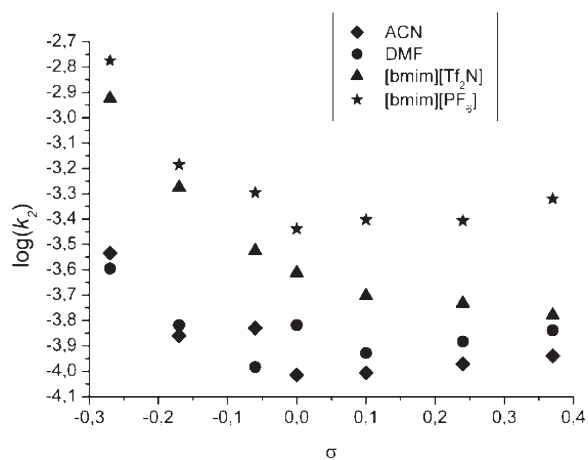


FIGURE 2. Hammett plots for the reaction between NMI and benzyl chlorides in organic solvents and ionic liquids at 333 K.

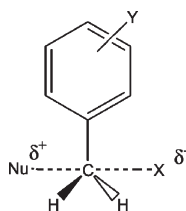


FIGURE 3. Transition state of a pure S_N2 mechanism.

chemistry, generally accepted is the existence of a continuous spectrum of mechanisms between S_N2 and S_N1 , as well as between S_N2 and S_NAr , arising from the progressive variation of the extent of bond formation and bond breaking at the carbon reaction center of the TS.^{19,20}

On this basis, the pure S_N2 mechanism represents a limiting situation characterized by a symmetric TS, i.e., bond breaking and making are simultaneous processes (Figure 3). This TS has a low charge density on the carbon reaction center, and the Hammett plots of reactions occurring through pure S_N2 mechanisms are generally straight lines with very low slopes, giving consequently low values of ρ . A shift of the mechanism toward S_N1 or S_NAr determines an increase of the asymmetric character of the TS. In particular, when bond formation is faster than bond breaking, the mechanism is still bimolecular but it resembles a S_NAr reaction, occurring through the formation of a carbanionic intermediate; this mechanism is called *tight* S_N2 and the corresponding Hammett plots are characterized by positive ρ values. On the other hand, if the bond breaking is anticipated with respect to the bond formation, the mechanism is called *loose* S_N2 and the Hammett plots give negative ρ values. A shift of the mechanism from *tight* S_N2 to *loose* S_N2 on going from EWS to EDS might therefore be the origin of the nonlinear Hammett plots found in the present study. It is, however, noteworthy that the behavior and slope of the plots related to the reactions in ILs are different from

those obtained in molecular solvents. In acetonitrile and [bmim][PF₆] the Hammett plots are composites of two straight lines; a linear correlation with negative slope ($\rho < 0$) can be found in the EDS range, while in the region of EWS the slope is positive. This means that, whereas a partial positive charge characterizes the activated complex when electron donating substituents are present (i.e., breaking of the C–Cl bond is faster than the C–Nu formation), with electron-withdrawing substituents the TS has a negative character. In [bmim][Tf₂N], the two straight lines have always negative slope and the behavior can be rationalized by considering that in going from EWS to EDS the breaking of the C–Cl bond becomes significantly faster than C–Nu bond formation and the activated complex acquires a higher partial positive charge.

Analysis of this latter data, considering the solvent effects emerging by the LSER approach, shows that in the presence of electron-donating substituents, which are able to support a positive charge at the carbon reaction center, the departure of the chloride ion precedes the bond formation. The mechanism is a loose S_N2 and the hydrogen bond donor ability of the IL becomes the main factor affecting the reaction rate. On the other hand, in the presence of electron-withdrawing substituents (or of a hydrogen atom), development of the positive charge is disfavored and the reaction occurs through TSs having a more symmetric character and the solvation effect is more complicated; a combination of effects must be considered to obtain a fairly good correlation.

Theoretical Calculations. To better define the role of the solvent on the reaction profile of benzyl chloride with *N*-methylimidazole, a theoretical investigation has also been performed. Unfortunately, the effects of ionic liquids on chemical reactions have not been rationalized enough to allow the development of a computational model that takes account of them efficiently and with a limited computational effort. In the past years several molecular dynamic studies, both classical and ab initio, of ILs have been performed.²⁰ In the specific case of the study of a chemical reaction, pure classical methods are not feasible because of the intrinsic quantum nature of chemical bond formation/breaking processes. We chose to use the supermolecular approach,²¹ including one or more ions in a model system. This is less computationally expensive than an ab initio molecular dynamics study and allows us to focus our attention on specific solute–solvent interactions. Using this approach, the Menshutkin reaction represents a unique situation since two neutral reagents lead to two ionic species: a chloride anion and an imidazolium cation. In the simplest neutral supermolecular approach, one ion pair representing the solvent phase and two neutral molecules that can form an additional ion pair are included in the model.

The computational study of the Menshutkin reaction between benzyl chloride and *N*-methylimidazole was therefore performed in vacuo, in 1,2-dichloroethane (DCE, a classic molecular solvent having a dielectric constant similar to many ILs) and with an explicit ionic pair, 1-butylimidazolium hexafluorophosphate ([Hbim][PF₆]). In all of the investigated situations, a scan along the natural reaction

(19) Richard, J. P.; Jencks, W. P. *J. Am. Chem. Soc.* **1984**, *106*, 1383. Bentley, T. W.; Schleyer, P. v. R. *J. Am. Chem. Soc.* **1976**, *98*, 7667. Bentley, T. W.; Schleyer, P. v. R.; Bowen, C. T.; Morten, D. H.; Schleyer, P. v. R. *J. Am. Chem. Soc.* **1981**, *103*, 5466.

(20) Wang, Y.; Jiang, W.; Yan, T.; Voth, G. A. *Acc. Chem. Res.* **2007**, *40*, 1193. Del Popolo, M. G.; Kohanoff, J.; Lynden-Bell, R. M.; Pinilla, C. *Acc. Chem. Res.* **2007**, *40*, 1156.

(21) Acevedo, O.; Jorgensen, W. L.; Evanseck, J. D. *J. Chem. Theory Comput.* **2007**, *3*, 132. Bini, R.; Chiappe, C.; Lloplis Mestre, V.; Pomelli, C. S.; Welton, T. *Theor. Chem. Acc.* **2009**, *113*, 347.

TABLE 4. Energetic Values for Reaction Paths Calculated at the B3LYP/CEP-121G(d,p) Level

R_{C-N} (Å)		relative energies (kcal/mol)			
		vacuo	DCE	IP low	IP high
1.50	a	7.97	-5.11	-15.47	-2.37
1.75		16.11	3.67	-5.18	8.14
2.00		28.09	16.81	10.67	23.14
2.18	b			13.04	
2.25	b	36.33	26.15	12.59	34.37
2.45	b				40.38
2.50		41.21	31.82	7.48	7.48
2.75		44.18	35.40	3.77	3.77
2.80		44.82			
2.98	b		38.54		
3.00		2.13	37.89	2.05	2.05
3.25		0.01	0.09	1.00	1.00
3.50		-0.43	-0.29	0.39	0.39
3.75		-0.35	-0.19	0.28	0.28
4.00		-0.17	-0.07	0.04	0.04
4.25		0.00	0.00	0.00	0.00

^aAbsolute minimum, the R_{C-N} values differ at the 3rd digit. ^bTransition states. An extended version of this table complete with absolute energies is available in Supporting Information.

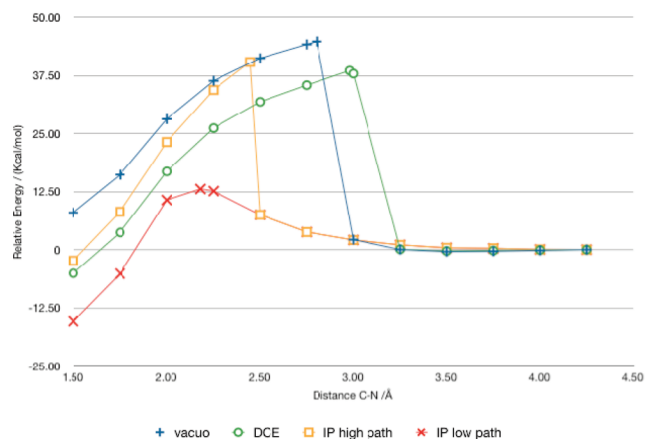
coordinate, defined as the distance between the *N*-methylimidazole nitrogen and the benzylic carbon (R_{C-N}), was performed. The standard choice of the infinite distance between the reagents as the reference state is not well-defined in this case. In particular, in the supermolecular system there is not a defined geometry at infinite distance. However, the computational results show that at a R_{C-N} distance of 4.25 Å all the reaction profiles are flat. Consequently, we decided to take this distance as the zero reference for the energy. In DCE, we used the continuum model IEFPCM with default parameters. All calculations were performed using the Gaussian 03 suite of programs,²² at B3LYP/CEP-121G(d,p) theory level. Several of the authors have successfully used this level of theory in previous work examining chemical reactivity in ionic liquids and in other contexts.²³

The results are reported in Table 4 and graphically represented in Figure 4.

For the reactions performed in vacuo and in DCE we started from the product with a nearby chloride ion. Starting from the product structure a relaxed scan was performed until the value of $R_{C-N} = 4.25$ Å was reached. The top point of each curve was taken as the starting point for a transition state structure optimization. In the model system containing an explicit ionic pair (IP), the supermolecule structure was obtained adding [Hbim]⁺ at the

(22) Frisch, M. J.; Trucks, G. W.; Schlegel, H. B.; Scuseria, G. E.; Robb, M. A.; Cheeseman, J. R.; Montgomery, J. A., Jr.; Vreven, T.; Kudin, K. N.; Burant, J. C.; Millam, J. M.; Iyengar, S. S.; Tomasi, J.; Barone, V.; Mennucci, B.; Cossi, M.; Scalmani, G.; Rega, N.; Petersson, G. A.; Nakatsuji, H.; Hada, M.; Ehara, M.; Toyota, K.; Fukuda, R.; Hasegawa, J.; Ishida, M.; Nakajima, T.; Honda, Y.; Kitao, O.; Nakai, H.; Klene, M.; Li, X.; Knox, J. E.; Hratchian, H. P.; Cross, J. B.; Bakken, V.; Adamo, C.; Jaramillo, J.; Gomperts, R.; Stratmann, R. E.; Yazyev, O.; Austin, A. J.; Cammi, R.; Pomelli, C.; Ochterski, J. W.; Ayala, P. Y.; Morokuma, K.; Voth, G. A.; Salvador, P.; Dannenberg, J. J.; Zakrzewski, V. G.; Dapprich, S.; Daniels, A. D.; Strain, M. C.; Farkas, O.; Malick, D. K.; Rabuck, A. D.; Raghavachari, K.; Foresman, J. B.; Ortiz, J. V.; Cui, Q.; Baboul, A. G.; Clifford, S.; Cioslowski, J.; Stefanov, B. B.; Liu, G.; Liashenko, A.; Piskorz, P.; Komaromi, I.; Martin, R. L.; Fox, D. J.; Keith, T.; Al-Laham, M. A.; Peng, C. Y.; Nanayakkara, A.; Challacombe, M.; Gill, P. M. W.; Johnson, B.; Chen, W.; Wong, M. W.; Gonzalez, C.; Pople, J. A. *Gaussian 03, Revision C.02*; Gaussian, Inc.: Wallingford, 2004.

(23) Chiappe, C.; De Rubertis, A.; Jaber, A.; Lenoir, D.; Wattenbach, C.; Pomelli, C. S. *J. Org. Chem.* **2002**, *67*, 7066. Chiappe, C.; Detert, H.; Lenoir, D.; Pomelli, C. S.; Ruasse, M.-F. *J. Am. Chem. Soc.* **2003**, *125*, 2864.

**FIGURE 4.** Relaxed scans versus the C–N distance.

structure of the product in DCE and optimizing the resulting system. The imidazolium cation docked with the chloride anion, interacting with the C2 proton and with the butyl group hydrogens. This structure is similar to others found for a similar study involving the Diels–Alder reaction and is one of the structures found by Hunt et Al for the BMIM-Cl ionic pair²⁴ docking.

Then, the ion pair anion ($[PF_6]^-$) was added. $[PF_6]^-$ does not represent a chemical moiety (like hydrogens on a charged heteroaromatic ring for $[Hbim]^+$) able to establish a directional interaction with the cation + products system; the main interaction is electrostatic. If we first place $[PF_6]^-$ near $[Hbim]^+$ and then near the positive charged product, two stationary points are found as shown in Figure 5. We stress that this procedure is not exhaustive but is based on a combination of chemical and electrostatic common sense.

The structure on the left is energetically less stable and looks like two ionic pairs ($[Hbim]Cl$ and $[PF_6]^-$ -product). The structure on the right is more stable and looks like four ions in a quadrilateral arrangement with alternating charges. Both of these structures have been taken as starting points for the relaxed scans. We refer to the corresponding pathways as IP-high path and IP-low path, with high and low related to the relative energetic stability. All of the four transition states were characterized with normal mode calculations. Transition vectors are represented graphically in Figure 6 and reported in Supporting Information.

A first analysis of digits and curves shapes (Figure 4) shows that in vacuo, in DCE, and in the IP-high paths a similar behavior can be evidenced: a flat tail on the right, a rapid slope up to the TS (the relative energies of the TS structures are 44.86, 38.54, and 40.38 kcal/mol, respectively) followed by a less rapid slope down from the TS to the products. The larger difference between the three reactions is in the reaction coordinate value of the transition states that are 2.80, 2.98, and 2.45 Å, respectively. In contrast, the IP-low path has a TS with a relative energy of 13.04 kcal/mol and a reaction coordinate of 2.18 Å. A visual inspection of the transition state geometries, reported in Figure 6, confirms the similarities of the first three structures and the diversity of the fourth one, related to the IP-low path. The IP-low path TS is the only one that shows a linear structure

(24) Hunt, P.; Kirchner, B.; Welton, T. *Chem.—Eur. J.* **2006**, *12*, 6762.

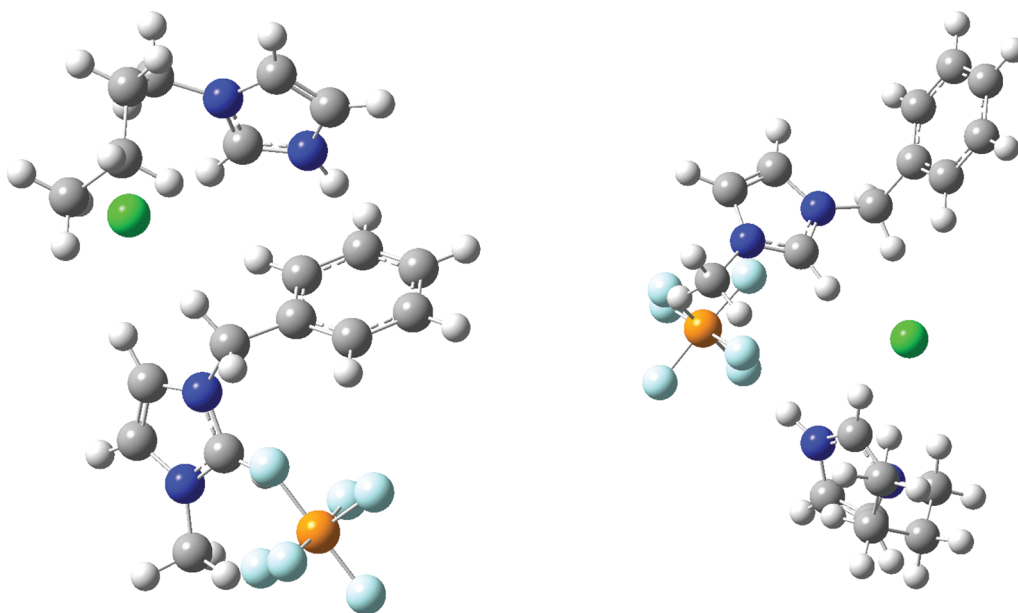


FIGURE 5. Two conformations found for the reaction product with an ionic pair. The structure on the left is the IP-high path, and that on the right is the IP-low path.

TABLE 5. Natural Atomic Charges Condensed to Significant Fragments of the Supramolecular System in the Various Reaction Paths

fragment	geometry	vacuo	DCE	IP-low path	IP-high path
Cl ⁻	reference	-0.150	-0.165	-0.203	-0.203
	transition state	-0.740	-0.839	-0.635	-0.848
	product	-0.870	-0.928	-0.881	-0.868
Φ-CH ₂ ⁺	reference	0.147	0.161	0.209	0.209
	transition state	0.687	0.811	0.440	0.706
	product	0.307	0.614	0.311	0.305
methylimidazole	reference	0.003	0.004	-0.003	-0.003
	transition state	0.053	0.028	0.226	0.227
	product	0.563	0.314	0.620	0.630
HBIM	reference			0.932	0.932
	transition state			0.910	0.884
	product			0.898	0.898
PF ₆ ⁻	reference			-0.935	-0.935
	transition state			-0.941	-0.969
	product			-0.948	-0.964

expected for a typical S_N2 reaction: the Cl-C-N angle is of 161.4°. Furthermore the IP-low transition vector is the only in which the chlorine atom is appreciably involved.

In the other reaction pathways angles are 100.1° for the IP-high path, 84.9° for the reaction in vacuo, and 88.1° for the reaction in DCE. Furthermore, the natural bond orbital (NBO) population analysis reported in Table 5 shows that the charge separation process is less extended in the IP-low TS than in the other cases, in agreement with a more synchronous S_N2 reaction. It is noteworthy that any attempt to find linear or nearly linear TSs for the reactions in vacuo and in DCE led directly to the angular structures reported in Figure 6. On the other hand, the atypical nonlinear TS and the propensity of those systems to give the angular structure may be considered a consequence of the nature of the product; imidazolium cation and a chloride anion surely do not easily form in vacuo and in low polar solvents. The pathways with a bent TS allow the developing charged species to find stabilization through electrostatic

interactions: chloride atom interacts with both reagents and the cationic moiety of the product. In the TSs related to the reaction in vacuo and in DCE, chloride finds its minimum energy position between the two reagents. However, we maintain that the bent mechanism is strongly determined by the reagent's nature and reaction conditions (selected medium). In agreement with this statement, recent calculations on the Menshutkin reaction between 2-amino-1-methylbenzylimidazole and iodomethane report²⁵ the expected linear transition state. Surely, the larger and more polarizable iodide stabilizes the negative charge better than chloride and consequently reduces the necessity to find intrinsic stabilization by interacting with the developing positive charge. Moreover, the interaction between iodide and the imidazolium cation is weaker than that of chloride with the same cation, as evidenced ESI-MS measurements.²⁶ Related to the solvent, although in both cases the same continuum solvent model has been used, in the more polar solvent (CH₃CN) ion pair dissociation is favored. Finally, it is noteworthy that in the reaction of 2-amino-1-methylbenzimidazole with iodomethane, the higher basicity of the nucleophile (a primary amine instead of an aromatic tertiary amine) and the lower steric requirements of the electrophile (a methyl derivative) might aid the more synchronous pathway.

Related to the effect of the ion pair on the reaction pathway, both the IP-high and IP-low TSs have the developing chloride coordinated to [Hbim]⁺ cation. This can be considered the primary effect of the presence of the ionic liquid on this reaction: it is able to transform an anionic leaving group (chloride) in an ion pair leaving group ([Hbim]Cl). The interaction of the IL cation with the leaving group does not necessarily affect the reaction pathway, the energetic and

(25) Melo, A.; Alfaia, A. J. I.; Reis, J. C. R.; Calado, A. R. T. *J. Phys. Chem. B* **2006**, *110*, 1877.

(26) Fernandes, A. M.; Coutinho, J. A. P.; Marrucho, I. M. *J. Mass Spectrosc.* **2008**, *44*, 144. Bini, R.; Bortolini, O.; Chiappe, C.; Pieraccini, D.; Siciliano, T. *J. Phys. Chem. B* **2007**, *111*, 598.

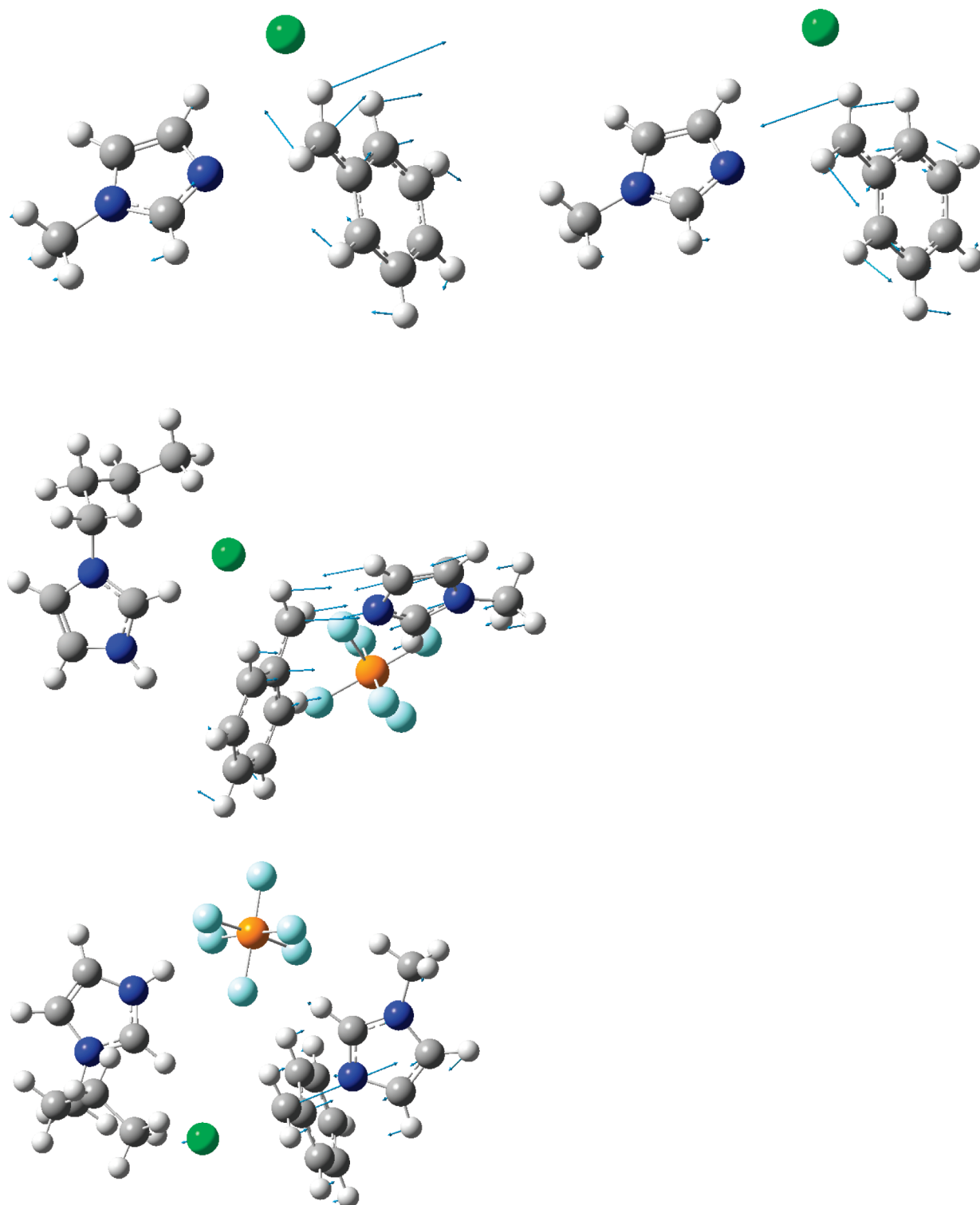


FIGURE 6. Similar bent TS structures found in vacuo (top left), in DCE (top right) and IP high-paths (middle). A different, nearly linear arrangement is found in the case of the IP high-path (bottom). The transition vectors are represented by arrows (phase and scale are arbitrary). The vector values are reported in Supporting Information.

geometry of the IP-high path is similar to those found for the two non-IP paths (i.e., vacuo and DCE). However, depending on the disposition of both the cation and anion with respect to the reagents, this interaction allows the leaving chloride to maintain a quasi-aligned position with respect to the formed C–N bond, reducing the TS energy. Furthermore,

the dipole orientation of the IP facilitates the charge-separation process. In the less favorable orientation (IP-high TS) the chloride-product interaction is weaker but not negligible: the Cl–C–N angle is about 10° larger than in non-IP TSs.

In our model system we have considered only two possible dispositions of the IP representing the IL, but the real liquid

consists in a large number of ions. Moreover, considering the inhomogeneous nature of ILs on the short time scale (Kerr effects suggest²⁷ an anion position change on the order of picoseconds) it is possible to hypothesize that inside the bulk liquid the two reagents are in contact with different solvation cages and the reaction can take place or not, depending on the relative disposition of the ionic liquid anions and cations with respect to reagents. The two situations reported here represent a more favorable and a less-favorable disposition of the cybotactic region around the reagents but we cannot claim that they represent the sole situations or the limiting situations. Probably, there are several possible reaction pathways for this reaction in ILs having different, but not extremely different, TS energies. A thermodynamic description of the transition state complex would require bond equilibrium to prorogate through both the IL and reactants during the lifetime of the transition state; but, IL conformational changes are slow. Consequently, thermodynamic equilibrium cannot occur at the transition state. However, IL cations and anions are present around the substrates before reaching the transition state and they remain close during the lifetime of the transition state. The dynamic motion of linked regions of the IL might transfer vibrational energy into the reacting system, favoring the appropriate alignment of reagents in a precomplex having the proper reagent disposition. On this assumption, the Menshutkin reaction of benzyl chloride with *N*-methylimidazole in ILs should be more realistically discussed in terms of multiple reaction pathways ranging from the classical synchronous S_N2 process to less concerted bent pathways with the overall reaction rate being the average of the reaction constants defining these processes.

Conclusions

In conclusion, the data reported here demonstrate that although the Menshutkin reaction gives ionic species starting from neutral compounds, the effect of the ionic environment is moderate. The reaction occurs in ILs as in molecular solvents by the expected bimolecular mechanism and an increase in reactivity going from aprotic polar solvents to ILs can be evidenced only with benzyl chlorides. By applying the Kamlet–Taft LSER approach to the kinetic data found for benzyl chlorides bearing EDS, it is possible to attribute this effect mainly to the ability of the IL to favor the chloride departure acting as hydrogen bond donor. On the other hand, the nonlinearity of the Hammett correlations suggest that on going from EWS to EDS the reaction mechanism changes from a pure S_N2 to a loose S_N2 mechanism, i.e., to a mechanism having a higher S_N1 character, and C–Cl bond breaking is faster than C–N bond making.

Finally, calculations performed using a model system in which the IL is represented by an explicit ionic pair (IP) confirms the primary role of the IL cation in the departure of the leaving group; however, the effect depends on the relative position of the IP with respect to the reagents. Two possible different reaction pathways have been obtained changing

this parameter: an unusual bent asynchronous S_N2 mechanism (found also in vacuo and DCE) and a quasi-linear synchronous mechanism. Considering the inhomogeneous nature of ILs on the short time scale (that of a TS), it is possible to hypothesize that inside bulk liquid the two reagents are in contact with different solvation cages and the reaction can proceed through different reaction pathways. The overall reaction rate becomes the average of the reaction rates of the single processes. The term “transition state stabilization” that has fostered the idea that an energy-equilibrated transition state exists cannot be used and “realistic IL transition states” might more appropriately be expressed in terms of statistical dynamic probabilities rather than thermodynamic expressions.

Experimental Section

Materials. Benzyl halides and substituted benzyl halides were purchased from commercial sources and used as received. *N*-Methylimidazole was dried and distilled over KOH under vacuum. Ionic liquids were synthesized using standard procedure and were dried under vacuum for 6 h at 80 °C before use. Organic solvents were purified and dried using standard procedures.

Kinetic Procedure. The Menshutkin reaction between *N*-methylimidazole and benzyl halides were carried out under pseudo-first-order conditions using an excess of *N*-methylimidazole (by a factor of 10 up to 100). All reactions were monitored within 0.1 mm quartz cuvettes using an UV–vis spectrometer following the decrease of absorbance of benzyl halides at appropriate wavelengths (normally 260–300 nm). In a typical experiment, a concentrated solution of benzyl halide was prepared in a 5 mL calibrated flask using CH₂Cl₂ as solvent. A proper amount of *N*-methylimidazole (exactly weighted) was added to 1 mL of the solvent, pre-thermostatted at the appropriate temperature (± 0.1 K) for 10 min, in a calibrated flask, and the solution was mixed manually until homogeneous. Then, 50 μ L of the concentrated solution of benzyl halide was added and the solution was rapidly transferred to the quartz cell. The kinetic data (absorbance/time) were fit to eq 1, and the obtained k_{obs} were plotted against the molar concentrations of *N*-methylimidazole in order to find the second order rate constants k_2 , which are reported in Tables 2 and 3. In selected reactions, products were identified by ESI-MS.

Theoretical Calculations. All calculations were performed using the Gaussian 03 suite²² (C.02 release) on the argo linux cluster of our department. The cluster is composed of number crunching servers based on Supermicro superserver barebones (6015 series) and Intel Xeon quad-core processors (54XX series). All servers are equipped with Kingston ECC RAM (certified for the motherboard) and Seagate (Barracuda 7200 series) SATA2 Hard Disks. The Linux version is CentOS 5.2.

Acknowledgment. The authors would like to thank the University of Pisa for the financial support.

Supporting Information Available: An extended version of Table 4 containing absolute energies, a table containing some geometrical quantities about the calculated structures, transition vectors for the four transition states reported in the paper (excerpts from Gaussian outputs), and molecular coordinates for all the structure reported in XYZ format. This material is available free of charge via the Internet at <http://pubs.acs.org>.

(27) Cang, H.; Li, J.; Fayer, M. D. *J. Chem. Phys.* **2003**, *119*, 13017.